

Study of Parametric Influence on Dry Sliding Wear and Corrosion Behavior of AA5754-TiB₂ In Situ Composites

K. Venkatasubbaiah,¹ K. Brahma Raju,² Ramki Alamanda,³ Ch. Suresh,⁴ K.E. Jagadish³

¹Andhra University, India

²SRKR College of Engineering, India

³Raghu Institute of Technology, India

⁴Avanathi Institute of Engineering and Technology, India

Abstract

Tribological properties determine the elemental factors influencing the performance of the components that are subjected to relative motion. Of late, low-density Metal Matrix Composites (MMCs) have been renowned as materials for the components that are subjected to tribological applications. This work reports an experimental study of wear and corrosion behavior of Aluminum Metal Matrix Composites (AMMCs) reinforced with in situ TiB₂ particles. These composites were synthesized by a mixed salt route procedure using K₂TiF₆ and KBF₄ at a temperature of 850°C by using the stir casting method. Dry sliding wear behavior of AA5754-TiB₂ in situ composites were compared with base material for the various loads, sliding speed, and sliding distances. These parameters were analyzed using Taguchi techniques. It was found that the percentage of reinforcement and load are the most significant parameters. Scanning Electron Microscopy (SEM) analysis was conducted on wear scars to find the wear mechanism. The corrosion behavior of in situ composites has been studied and compared with the base material. Potentiodynamic polarization tests were carried out to determine the corrosion resistance.

History

Received: 31 Dec 2019
 Revised: 30 Mar 2020
 Accepted: 02 Jul 2020
 e-Available: 29 Jul 2020

Keywords

Aluminum metal matrix composites, In situ, TiB₂, Wear, Coefficient of friction (COF), Corrosion, Taguchi

Citation

Venkatasubbaiah, K., Raju, K., Alamanda, R., Suresh, Ch. et al., "Study of Parametric Influence on Dry Sliding Wear and Corrosion Behavior of AA5754-TiB₂ In Situ Composites," *SAE Int. J. Mater. Manuf.* 13(3):2020, doi:10.4271/05-13-03-0021.

ISSN: 1946-3979
 e-ISSN: 1946-3987

This article is part of a Special Issue on Lightweighting Materials for Automotive Applications.



1. Introduction

In recent years, the investigation has been shifted to composite materials from undiversified materials to meet the global demands for lightweight and better performance materials. High specific strength, wear resistance, excellent dimensional stability, superior damping capacity, tribological behavior, good formability, and ability to exhibit superior strength-to-weight ratio and strength-to-cost ratio have driven the marine and aviation sectors and automobile, food, and mineral processing industries toward the new lightweight structural materials [1, 2, 3, 4]. It is widely thought that the use of aluminum in automotive manufacturing is a result of recent trends in development; however, constructing lightweight cars using modern, revolutionary materials such as aluminum looks back over a century. However, though most car manufacturers prefer steel today, due to rising consumer demand and new legal requirements about fuel consumption and environmental safety, OEM automakers have also increased weight-reduction attempts. Aluminum can be seen as a possible engineering alternative in this respect: its density is only about one-third of steel and aluminum alloys of specific high strength meet the torsion and rigidity requirements of an automobile component. The highly formable 5XXX alloys are currently used primarily for internal panel applications [5,6]. The automotive industry has focused on reducing fuel consumption and gas emission and tended to employ lightweight and economic materials. Al-Mg (AA5754) alloy is widely used in the inner body and trims panel, due to its good deformability. For car body applications, pressure vessels, and ships, AA5754 alloy is an important candidate and has thinner gauges than the plate thickness of about 6 mm usually used in other quoted reports [7,8]. When Al-Mg alloys are reinforced with hard and tough particles, there is a significant improvement in both mechanical as well as tribological properties, based on suitable combinations of processing techniques, and matrix and reinforcement combinations, which in turn increases their usage in multiplicity applications. These being particulate composites, being a class of metal matrix composites (MMCs), take lavish attention in diverse sectors such as automobile, marine, and aviation because of their lightweight, castability, economical, immense wear resistance, and isotropic properties [9]. Thus, Al-Mg alloys are becoming more important in this aspect as Mg offers a high strength-weight ratio, good castability, and excellent deep drawing and stretch behavior.

The manufacturing of composites is commonly done by diverse methods, although traditionally enhanced AMMCs has been produced discontinuously in several “ex-situ” techniques Collocation reaction between the matrix phase and dispersion phase and destitute wettability due to surface contamination of the reinforcement are noticed as the common limitations of these composites. The potential way to mitigate these is by using the in situ process whereby desired clean dispersoids can be homogeneously dispersed. This technique is a novel technique developed to fabricate AMMCs for better adhesion and mechanical properties [10,11]. The molten aluminum alloy was reinforced with ultrafine ceramic particles through in situ

process. Uniform distribution, fine-sized particle reinforcement, thermodynamically stable, and clear interface formation can be obtained through this technique [12].

Many researchers studied the wear behavior of aluminum composites with different weight/volume percentages of TiB₂ formed by the mixed salt route method technique. It was found that the formation/presence of Al₃Ti phase along with TiB₂ results in wear loss of the composites [13, 14, 15]. It is therefore important to control the formation of the Al₃Ti phase during the synthesis of in situ Al/TiB₂ composites in order to have good wear and mechanical properties. Among all the existing techniques in synthesizing Al-Si/TiB₂ [16, 17, 18, 19], in situ is most advantageous as it can control the phases, with minimal contamination and the possibility of bulk, and continues casting.

It was observed that Al-4Cu/TiB₂ in situ composite's abrasive wear resistance was compared with matrix alloy resistance. Due to the suppression of the intermetallic Al₃Ti phase, the wear performance of AMMCs was improved [20,21]. In situ synthesized Aluminum-Titanium Di-boride composite exhibits good mechanical properties without ductility loss [22] and has excellent dry sliding [21] and abrasive wear resistance [20] compared to the base material. There was a proper distribution of both the particulates in the composite. The interface of the particulates was reaction free and exhibited good interfacial bonding. Mechanical properties of the in situ composites indicated that increasing the amount of reinforcement from 4 wt.% to 6 wt.% will lead to an increase in the UTS, YS, and hardness [23,24].

Radhika et al. [25] reported that output is influenced by multiple variables. The Taguchi technique is the best technique to formulate and detect the optimum combination of parameters for a given response. Sahin [26] investigated the abrasive wear behavior of AA2014-15 wt.% SiC composite by L9 Taguchi design and used analysis of variance (ANOVA) to analyze the wear parameters. Koksai et al. [27] adopted L9 Taguchi orthogonal array to obtain minimum wear levels for the input parameters load, sliding velocity, reinforcement ratio, and sliding distance in the preparation of Al/AlB₂ composite. Satpal et al. [28] used the Taguchi technique to identify the dry sliding wear behavior of Al-SiC-Al₂O₃-Graphite hybrid composite to identify the influence of the process parameters. Uvaraju and Natarajan [29] used the Taguchi technique and identified that the volume of reinforcement is an imperative factor, followed by other factors like load, speed, and time for friction and wear behavior of Aluminum 7075-SiC-B₄C composites. Lekatou et al. [30] developed AMMCs by adding TiC and WC submicron-sized particles, which controlled the corrosion of the alloy matrix evident from potentiodynamic polarization curves.

Given the above facts, the present work is taken up with the objective of studying the various process parameters that are affecting the dry sliding wear behavior of AA5754-TiB₂ in situ composites, using the Taguchi technique. It is also aimed to discover the optimum level of operating parameters under test circumstances to minimize material loss. The present investigation also aimed to study the corrosion behavior of these composites.

TABLE 1 Quantity of halide salts of K_2TiF_6 and KBF_4 for obtaining various compositions of materials.

Material composition	Quantity of powders added in "g"	
	K_2TiF_6	KBF_4
AA5754-0 wt.% TiB_2	0	0
AA5754-2.5 wt.% TiB_2	109.21	113.95
AA5754-5.0 wt.% TiB_2	218.42	227.9
AA5754-7.5 wt.% TiB_2	327.63	341.85

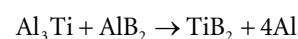
© SAE International

2. Materials and Methods

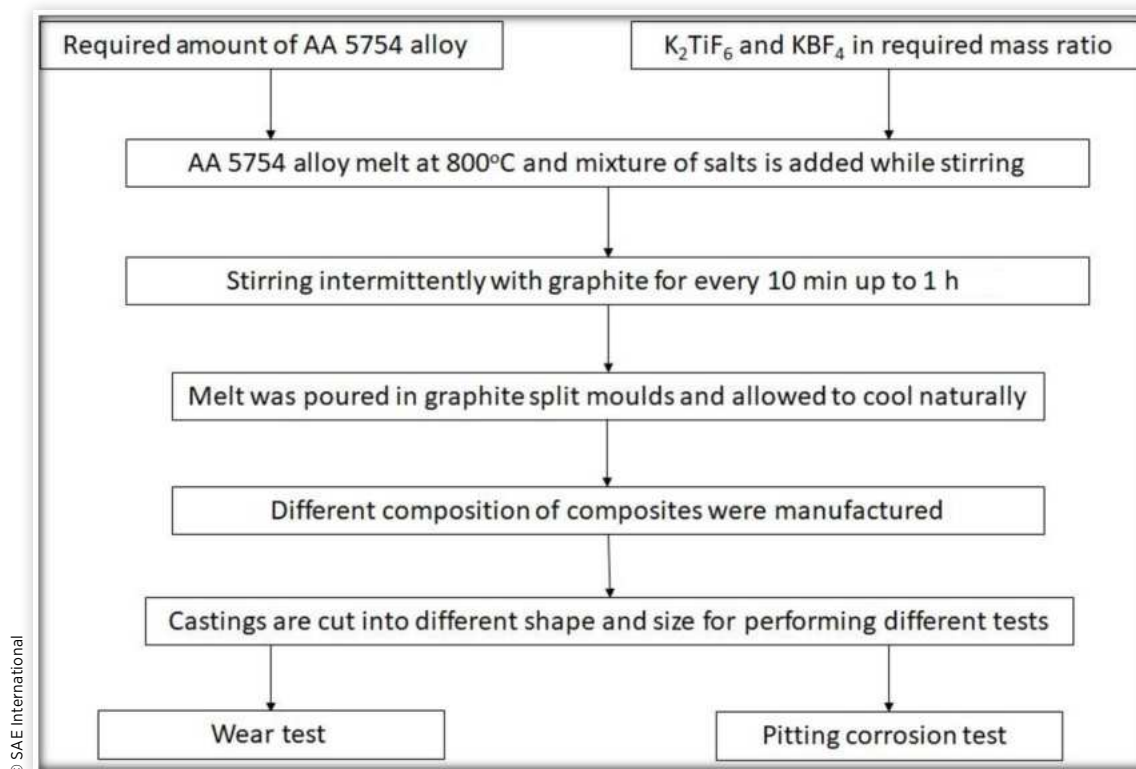
2.1. Fabrication of In Situ Composites

Al-Mg (AA5754) alloy was chosen as the matrix alloy, owing to its good corrosion resistance and mechanical properties. The chemical composition of the alloy (wt.%) is Mg 2.6 to 3.6, Cr 0.3, Cu 0.1, Fe 0.4, Mn 0.5, Si 0.4, Zn 0.2, and balanced Al. Initially calculated weight of AA5754 was kept in a graphite crucible and allowed to melt inside an electrical resistance stir casting furnace maintained at 800°C. To obtain composite having different wt.% of TiB_2 reinforcement (2.5, 5, and 7.5 wt.%) by in situ casting technique, the appropriate weights of halide salts K_2TiF_6 and KBF_4 to be added are stoichiometrically calculated (Ti/B ratio at 2.2:1) and the same is given in Table 1.

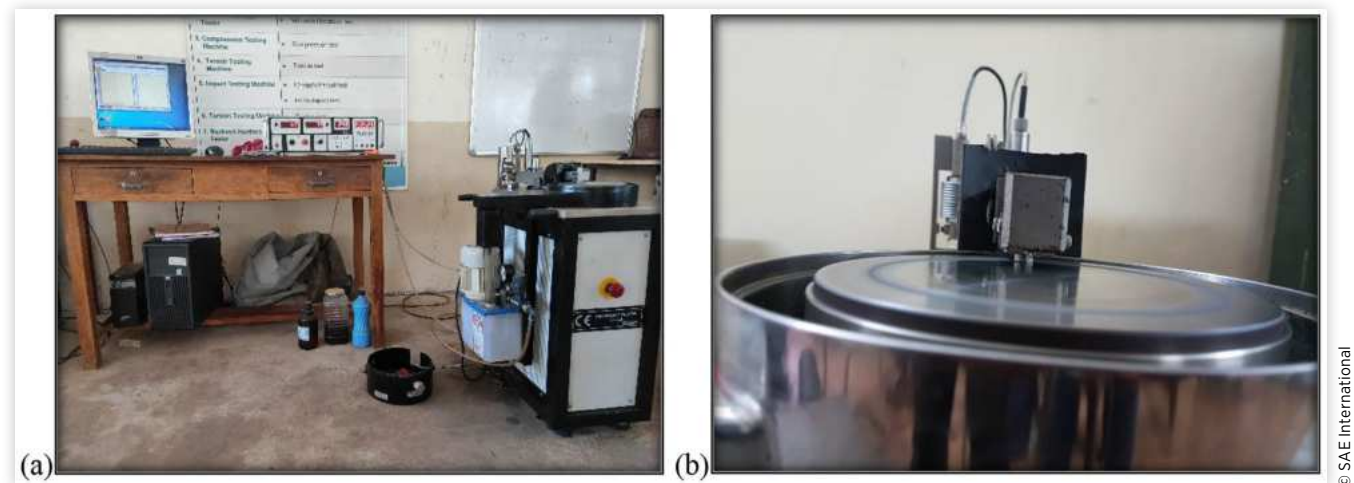
The determined quantity of halide salts is added at 800°C in the aluminum melt and well stirred to disperse the salt uniformly in the melt. The exothermic reaction between the in situ salts yield formed TiB_2 particles that are distributed uniformly in the alloy. The speed-regulated motorized stirring system with stirring rod and stirring blades, both made of mild steel coated with Zirconia, was mounted to the furnace to provide adequate mixing of halide salts in the aluminum melt. The mild steel stirrer was coated with zirconium to avoid possible contamination of the molten metal with iron. Stirring was continued for every 10 min up to 1 hour so that the interface between the particles and matrix promotes better wetting and finely dispersed particles. C_2Cl_6 was used for degassing [4]. The exothermic reaction pertained to the above process is as follows:



During the reaction, gases and slag were evolved. Before pouring the melt into the dies, the slag with low densities was decanted [3]. Gases that evolved during the reaction are liberated. The melt was poured in graphite split molds. Figure 1 shows the flowchart for synthesizing the composites, and the details of process parameters, microstructures, and mechanical characteristics are mentioned in an earlier work by the

FIGURE 1 Flowchart for synthesizing the composites.

© SAE International

FIGURE 2 (a and b) Pin-on-disk wear testing machine.

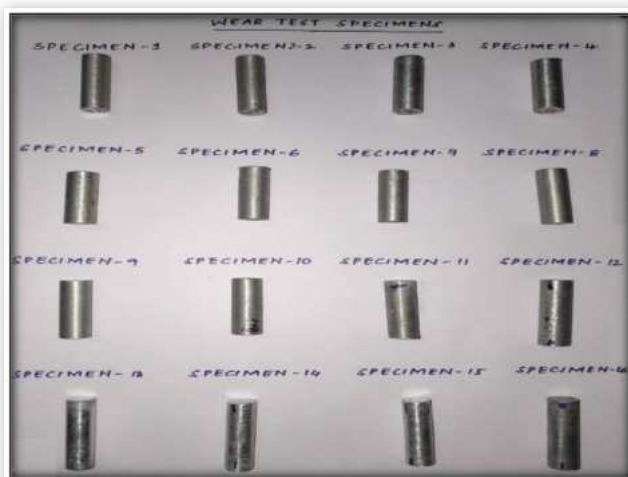
present authors [4]. Castings are obtained and they are cut into different shapes and sizes for performing different tests according to their standards. Through the article, the master alloy AA5754 was again casted without adding halide salts, which is further referred to as AA5754-0 wt.%.

2.2. Wear Test

Figure 2 shows the pin-on-disk wear testing equipment used to study the dry sliding wear behavior of the composite, which was conducted in dry laboratory conditions as per the ASTM G99-95 standard. The size of the pin was 10 mm in diameter and 40 mm in length, as shown in Figure 3. The counterpart disk with 160 mm for the outside diameter and 12 mm in thickness was fabricated using hardened EN 31 chromium steel with a hardness of 60 HRC and Ra value of 0.6 mm. The test specimens were loaded against the disk with a dead

weight. The specimens were cleaned with alcohol and weighed carefully using a 0.001 gm accuracy electronic balance, both before and after the tests. The difference between the initial and final weights was taken as a measure of slide mass loss. Literature states the percentage of reinforcement, load applied, sliding speed, and sliding distance are the influential process parameters to identify the wear rate in dry sliding conditions.

During the experiment, by applying the load, the pin specimen was pushed against the rotating disk. To study the pin's wear behavior, the wear-free counterpart was selected in such a fashion that it possesses higher hardness than the pin. To study the wear behavior of these composites, the end faces of these specimens and the counterpart were kept completely smooth so that pin-disk contact is achieved. The surface roughness of the rotating disk is close to 1 mm. Before and after the experimentation process, the counterpart disk was cleaned with acetone and later dried. The difference in weights after the experimentation process was measured using an electronic balance (Least Count = 0.001 g). These wear tests were performed by altering various process parameters. The samples were weighed after each test to determine the wear rate in terms of weight loss. The wear tests were carried out with variable sliding velocity, sliding distance, load, and reinforcement. Finally, the worn surfaces were observed under SEM to investigate the wear mechanisms.

FIGURE 3 Specimens for the wear test.

2.3. Experimental Design

Wear tests on AA5754-TiB₂ in situ composites were performed to analyze the influence of process parameters to find the Wear Rate (WR) and Coefficient of Friction (COF). L16 Taguchi experimental plan was chosen (Table 3), a standard array for the statistical analysis. The experimental results were converted into a signal-to-noise ratio (S/N) in Taguchi's design process. In this study, the characteristic performance was measured in terms of WR and COF. Taguchi's characteristics the lower the better performance was chosen. Characteristic

TABLE 2 Levels of process parameters.

Control factors	Units	Levels			
		1	2	3	4
% of reinforcement (A)	wt.%	0	2.5	5	7.5
Load (B)	N	10	20	30	40
Sliding speed (C)	m/s	1.5	3	4.5	6
Sliding distance (D)	M	1000	1500	2000	2500

© SAE International

performance is expected to be minimum. For every level of process parameters, S/N ratios were evaluated. Statistically significant parameters were determined using ANOVA. Finally, optimal combinations of test parameters were evaluated. The process parameter levels are shown in [Table 2](#). There are four levels in each control factor. The influences of the factors on tribological behavior were also studied.

3. Results and Discussions

3.1. Statistical Analysis

3.1.1. Influence on Wear Parameters on Wear Behavior Using Design of Experiments (DoE)

DoE is an effective method to find both the individual and interaction effects of various factors affecting the given process. ANOVA is carried out in order to execute the validity of the proposed parameters and to go beyond the significant factors. Based on the literature, load, sliding speed, sliding distance, and percentage of reinforcement were used as process parameters for the experimentation. Among these process parameters, the first three are process variables, while the percentage of reinforcement is a material parameter. The experimentation process was carried out in dry sliding conditions. DoE determines the proper combination of the process parameters and the specimens that are required for conducting the experiments. An L16 orthogonal factor design was selected for the present study. Statistical WR and COF analysis of Al-TiB₂ in situ composites is performed by conducting S/N ratio analysis and ANOVA. Taguchi recommended using S/N ratio instead of simple averages of experimental outcomes to obtain optimality, as S/N ratio assessment can study the variability of experimental outcomes under experimental circumstances. The WR and COF, which are considered as the objective function, are converted into S/N ratios, which are regarded as quality characteristics. Taguchi's "the lower the better" quality characteristics are being chosen to minimize the objective function.

3.1.2. Effect of Load, Sliding Speed, and Reinforcement on WR and COF

Four distinct loads, 10 N, 20 N, 30 N, and 40 N, were taken during wear trials to assess the composite's wear behavior. From the mean effect

plot, it can be seen that any increase in the load applied results in an increase in the WR and COF, which was similar to the results of Kumar [31]. The interface temperature had increased due to increased contact pressure, resulting in a higher rate of material removal due to increased load increases. As the load applied increases, more energy is converted as heat energy; adhesion occurs due to frictional heating, primarily due to increased removal of material. It can be noted that, with increased sliding speed, the WR decreases. The reduction of WR and COF is mainly due to the formation of the oxide layer that prevents direct contact between the sliding interfaces.

Increasing the weight fraction of TiB₂ content leads to wear rate reduction, owing to the high hardness of TiB₂, and leads to significant improvement in wear resistance. The increase in synthesizing TiB₂ in the composites increases the load-carrying capacity of the composites. This in turn increases the hardness of the composites serving these materials to reduce the WR and COF of the matrix alloy.

3.1.3. Analysis of Factors [Table 3](#) shows the S/N ratios calculated using Minitab 16, for analyzing the effect of factors that influences the WR and COF for all the experimental trials. [Table 4](#) and [Table 5](#) depict ANOVA and delta values that are derived from S/N ratios for every individual factor. These values determine factors influencing the WR in a systematic and orderly manner from high to low. The order of influencing factors from high to low are as follows: (1) percentage of reinforcement, (2) load, (3) sliding speed, and (4) sliding distance, respectively.

The optimum level of each control factor can be easily determined from the graph by considering "the lower the best" performance characteristics. [Figure 4](#) suggests the optimum conditions for minimum WR of the combinations A3B1C2D3 levels of the respective control factors. This clearly makes us understand that to reduce the wear rate of the composites, applied load and sliding speed have to be lowered and the percentage of reinforcement has to be increased. From the graph, it is clear that the wear rate is greatly influenced by the load compared with other factors. From previous studies, it has been evident that load is the critical factor controlling the wear behavior, which was indicated by Koksal [32]. It was reported that the wear rate increases with increasing load. The next influencing factor for wear rate is sliding speed. In general, the wear rate of matrix alloy increases with sliding speed. Kumar et al. [33] also reported that the wear rate increases with the sliding speed.

The most effective parameter for the decrease in wear rate is the percentage of reinforcement. The wear rate of composites has been observed to decrease with increased content of TiB₂ in the matrix. However, for a given percentage of reinforcement, the composite possesses a lower wear rate than the base material. The improved wear resistance of the composite with increased content of TiB₂ reinforcement can be attributed to the improvement of the hardness of the material. It has been clearly observed that the presence of ceramic reinforcements improves the wear resistance of the aluminum matrix alloys. The main effect plot also shows that the WR has a strong

TABLE 3 Experimental design using L₁₆ orthogonal array.

Experiment no.	% of reinforcement	Load	Sliding speed	Sliding distance	Wear rate	S/N ratio	COF	S/N ratio
1	0	10	1.5	1000	3.642233	-11.227	0.387	8.245
2	0	20	3	1500	3.99572	-12.031	0.422	7.493
3	0	30	4.5	2000	4.446822	-12.961	0.435	7.23
4	0	40	6	2500	5.397895	-14.644	0.452	6.897
5	2.5	10	3	2000	3.0173	-9.592	0.329	9.656
6	2.5	20	1.5	2500	3.613697	-11.159	0.352	9.069
7	2.5	30	6	1000	4.182391	-12.42	0.399	7.980
8	2.5	40	4.5	1500	4.517567	-13.09	0.405	7.850
9	5	10	4.5	2500	2.342429	-7.393	0.251	12.006
10	5	20	6	2000	2.812199	-8.980	0.283	10.964
11	5	30	1.5	1500	2.650338	-8.466	0.341	9.344
12	5	40	3	1000	2.687355	-8.586	0.35	9.118
13	7.5	10	6	1500	3.451995	-10.76	0.191	14.379
14	7.5	20	4.5	1000	3.570894	-11.05	0.227	12.879
15	7.5	30	3	2500	3.576042	-11.06	0.23	12.765
16	7.5	40	1.5	2000	3.597289	-11.11	0.247	12.146

© SAE International

influence on the percentage of reinforcement followed by load and sliding speed.

Table 6 and Table 7 depict ANOVA and delta values that are derived from S/N ratios for every individual factor. These values determine factors influencing the COF in a systematic and orderly manner, from high to low. The order of influencing factors from high to low are as follows: (1) percentage of reinforcement, (2) load, (3) sliding distance, and (4) sliding speed, respectively. Using the main effects plot and interaction plot, the influence of each design factor on the COF can be analyzed. The optimum level of each control factor can be easily determined from the graph by considering “the lower the best”

performance characteristics. Figure 5 suggests the optimum conditions for the minimum COF of the combinations A4B1C4D4 levels of the respective control factors. It is scrutinized that the COF for reinforced material is higher than that of base material due to adhesive wear behavior of the matrix material. Composite with 7.5% reinforcement has lower COF when compared to other reinforcement percentages. It is due to the fact that, when the particles are exposed during sliding, the real contact area of the lower percentage reinforced composite is low when compared to the higher percentage reinforced composite. As percentage reinforcement increases, the COF also increases proportionally due to the increase in

TABLE 4 ANOVA for S/N ratios of wear rate.

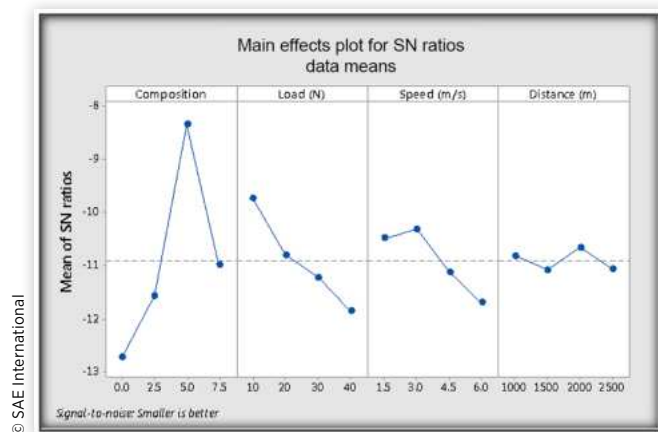
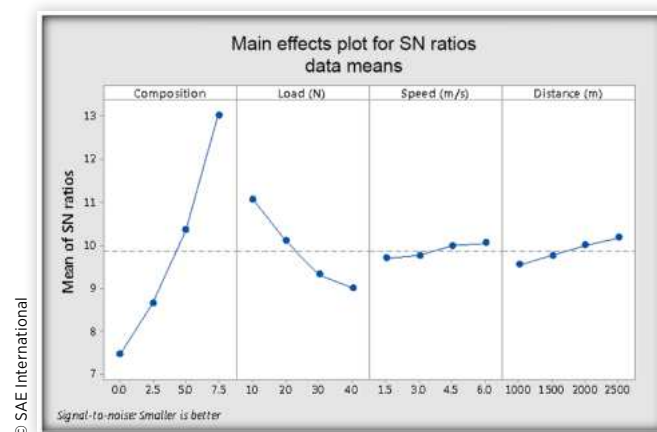
Source	DF	Seq SS	Adj MS	F	P	% contribution
% of reinforcement	3	70.3775	23.4592	384.29	0.000	85.84
Load (N)	3	10.1630	3.3877	55.49	0.004	12.39
Speed (m/s)	3	0.3593	0.1198	1.96	0.297	0.43
Distance (m)	3	0.8982	0.2994	4.90	0.112	1.09
Residual error	3	0.1831	0.0610			
Total	15	81.9812				

© SAE International

TABLE 5 Response table for wear rate S/N ratios (smaller is better).

Level	% of reinforcement A	Load (N) B	Sliding speed (m/s) C	Sliding distance(m) D
1	-12.716	-9.744	-10.493	-10.824
2	-11.569	-10.807	-10.320	-11.089
3	-8.357	-11.231	-11.127	-10.663
4	-11.001	-11.862	-11.704	-11.066
Delta	4.359	2.119	1.384	0.426
Rank	1	2	3	4

© SAE International

FIGURE 4 Main effects plot for wear rate on AMMC's S/N ratio.**FIGURE 5** Main effects plot for COF on AMMC's S/N ratio.

the real contact area and also due to the increase in wear debris entrapped between the sliding surfaces.

3.2. ANOVA Analysis

To find out the significance of the parameters on the WR, a statistical tool ANOVA is used. From ANOVA, S/N ratios of WR are depicted in Table 4, with computed R-Sq of 97.91%. Composition and Load are keyed out as the significant parameters with 85.84% and 12.39% contribution, respectively. The parameters such as sliding speed and sliding distance are found to be insignificant parameters on the WR with very low percentage contributions.

From ANOVA, S/N ratios of COF are depicted in Table 6, with computed R-Sq of 98.88%. Composition and Load are keyed out as the significant parameters with 86.03% and 12.42% contribution, respectively. The parameters such as sliding distance and sliding speed are found to be insignificant parameters on the COF with very low percentage contributions.

3.3. Correlation

Percentage of reinforcement and load are the effective factors, and quality characteristics (specific WR) are correlated by a multiple linear regressions. This is represented by correlation equations as follows:

$$\begin{aligned} WR = & 3.5939 + 0.7768 A1 + 0.2389 A2 - 0.9708 A3 \\ & - 0.0448 A4 - 0.4804 B1 - 0.0958 B2 + 0.1200 B3 \\ & + 0.4561 B4 - 0.2180 C1 - 0.2748 C2 + 0.1255 C3 + 0.3672 C4 \end{aligned}$$

$$\begin{aligned} COF = & 0.33131 + 0.09269 A1 + 0.03994 A2 - 0.02506 A3 \\ & - 0.10756 A4 - 0.04181 B1 - 0.01031 B2 + 0.01994 B3 \\ & + 0.03219 B4 + 0.00044 C1 + 0.00144 C2 - 0.00181 C3 \\ & - 0.00006 C4 + 0.00944 D1 + 0.00844 D2 \\ & - 0.00781 D3 - 0.01006 D4 \end{aligned}$$

TABLE 6 ANOVA for S/N ratios of COF.

Source	DF	Seq SS	Adj MS	F	P	% contribution
% of reinforcement	3	70.3775	23.4592	384.29	0.000	85.85
Load (N)	3	10.163	3.3877	55.49	0.004	12.40
Speed (m/s)	3	0.3593	0.1198	1.96	0.297	0.44
Distance (m)	3	0.8982	0.2994	4.9	0.112	1.10
Residual error	3	0.1831	0.061			
Total	15	81.9812				

TABLE 7 Response table for COF S/N ratios (smaller is better).

Level	% of reinforcement A	Load (N) B	Sliding speed (m/s) C	Sliding distance(m) D
1	7.467	11.072	9.701	9.556
2	8.639	10.102	9.758	9.767
3	10.359	9.33	9.992	9.999
4	13.043	9.003	10.055	10.185
Delta	5.576	2.069	0.354	0.628
Rank	1	2	4	3

3.4. Analysis of Wear Surface and Debris

Characterization of AMMCs, specifically worn surface microstructure, is more perplexed than the metals and alloys. To disseminate and analyze the mechanism of wear of AMMCs, SEM analysis of wear surface and wear debris formed during the process was studied. Figure 6 shows the low magnification of SEM micrographs of master and in situ composites that are tested at 40 N. From Figure 6(a), a unique pattern of grooves and ridges can be observed that are running parallel to each other in the master composite AA5754-0 wt.% TiB₂. Figures 6(b), (c), and (d) exemplify that grooves in in situ composites are much shallower than the master composite AA5754-0% TiB₂ grooves because of the existence of TiB₂ particles. Extravagantly from Figure 6(c), grooves are much finer, tightly spaced owing to their sliding action of debris and tough particles in AA5754-5 wt.% TiB₂. Furthermore, the

examination of the master alloy AA5754-0 wt.% TiB₂ alloy's trailing edge shows a gross plastic deformation attributed due to the lack of in situ particles [Figure 6(a)], whereas in the in situ composites demonstrates gentle edge profile [Figure 6(b), (c), and (d)]. Some patches of oxygen-rich material are also observed, which are evenly distributed across the worn surface and eventually break off to form the loose debris.

Figure 7(a) to (d) show the high magnification of SEM micrographs of composites that are tested at 40 N. In the case of master composites, the deformation range is quite high [Figure 7(a)]; whereas in situ, a composite demonstrates fewer and smaller cracks [Figure 7(b), (c), and (d)].

The extent of the wear debris produced has an immense impact on the in situ composites in terms of WR and COF. The present work exhibits the size and morphology of the wear debris. They are distinctly different and largely depend upon the load and the formation of TiB₂ particles. SEM micrographs shown in Figure 8(a) and (b) depict coarse flaky and fine

FIGURE 6 (a) 0 wt.%, (b) 2.5 wt.%, (c) 5 wt.%, and (d) 7.5 wt.% SEM images (lower magnification) of wear surfaces of AA5754-TiB₂ in situ composites at 40 N load.

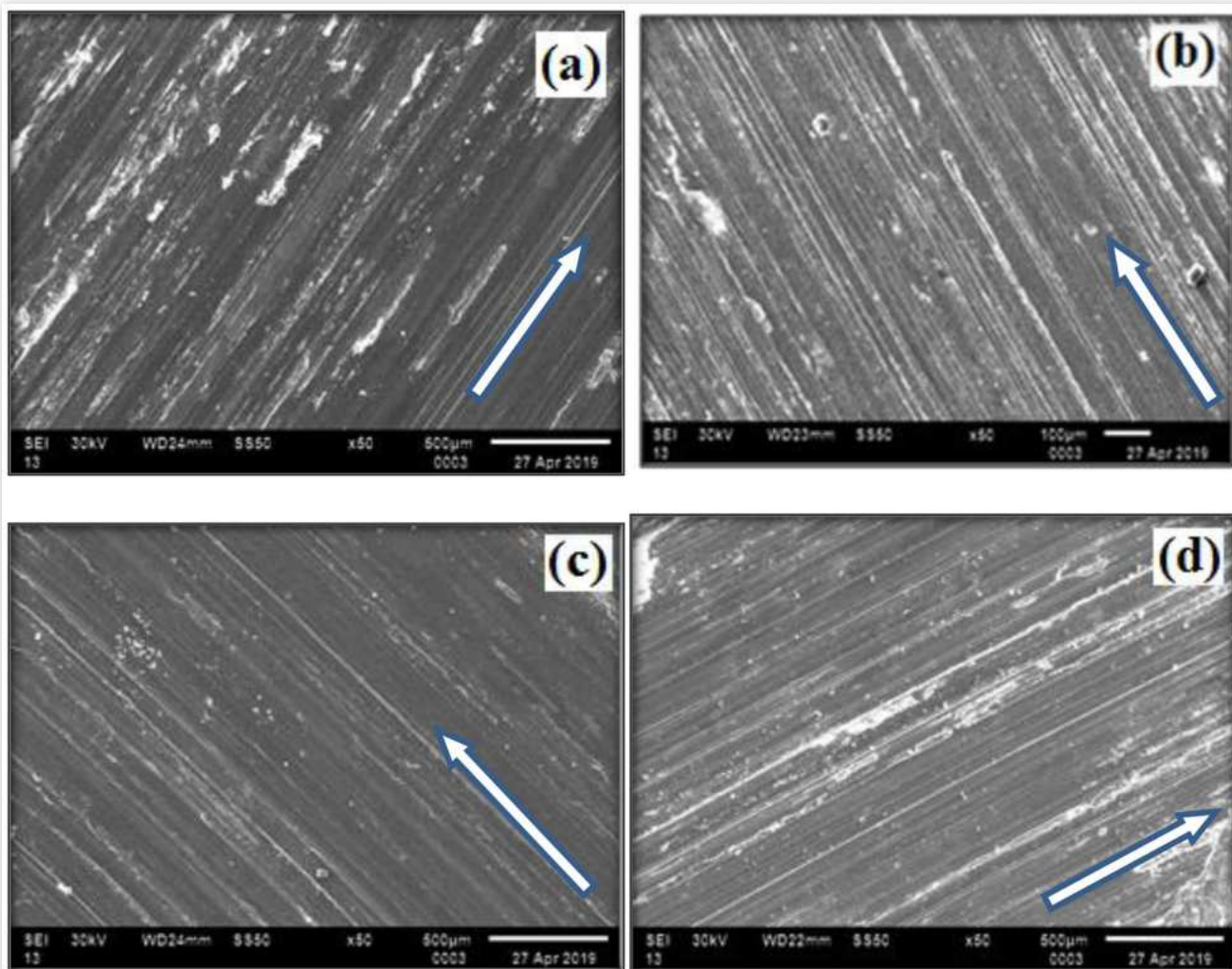
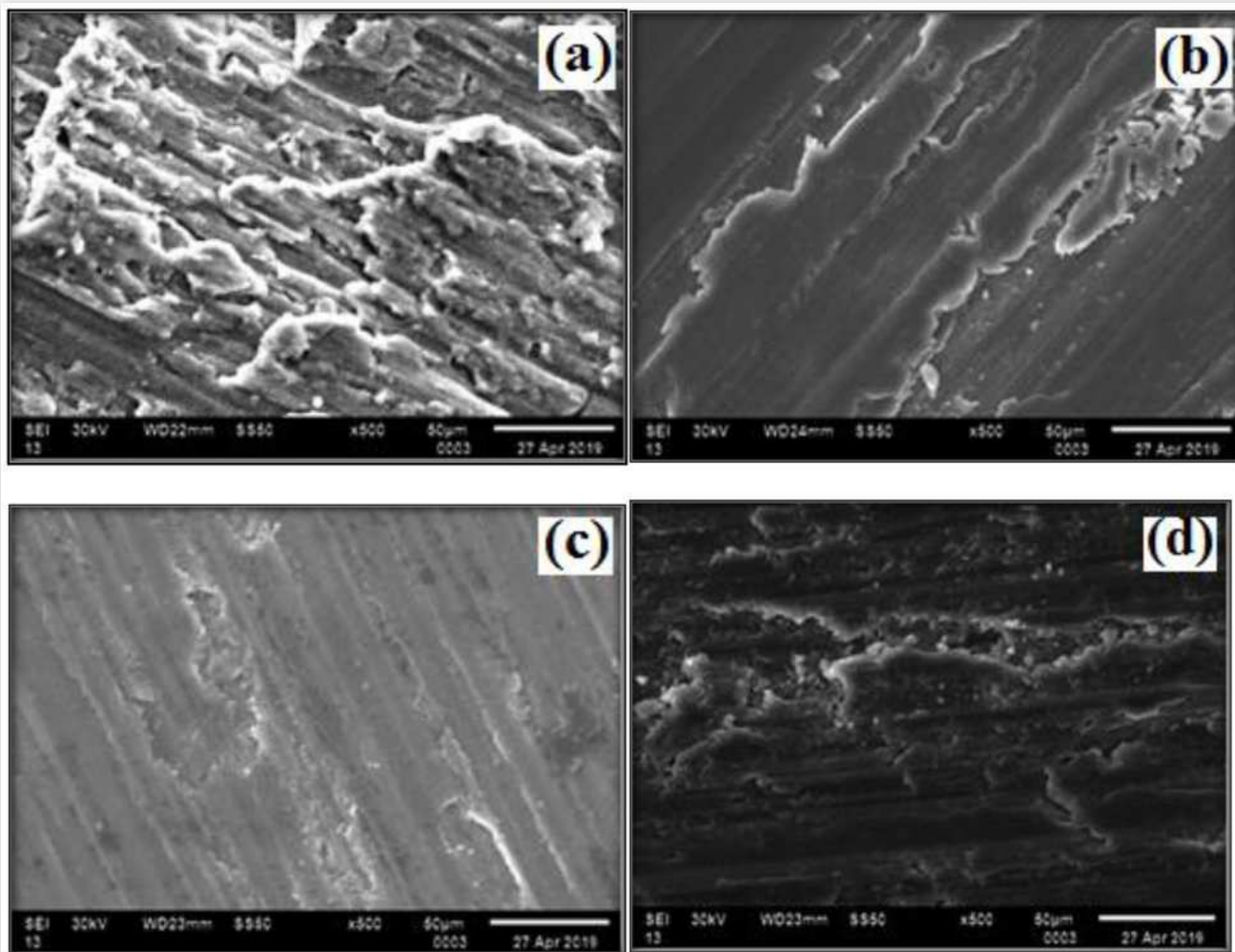


FIGURE 7 (a) 0 wt.%, (b) 2.5 wt.%, (c) 5 wt.%, and (d) 7.5 wt.% SEM images (higher magnification) of wear surfaces of Al5754-TiB₂ composites at 40 N.



© SAE International

equiaxed debris that is produced during the sliding wear. The fine fragments are known to be the most numerous regardless of the actual load [1]. As the load enhances from 10 to 40 N, the quantity and size of the flaky debris increases, which indicates the delamination of wear mechanism. Figure 8(d) demonstrates the existence of both longitudinal and transverse cracks within the debris.

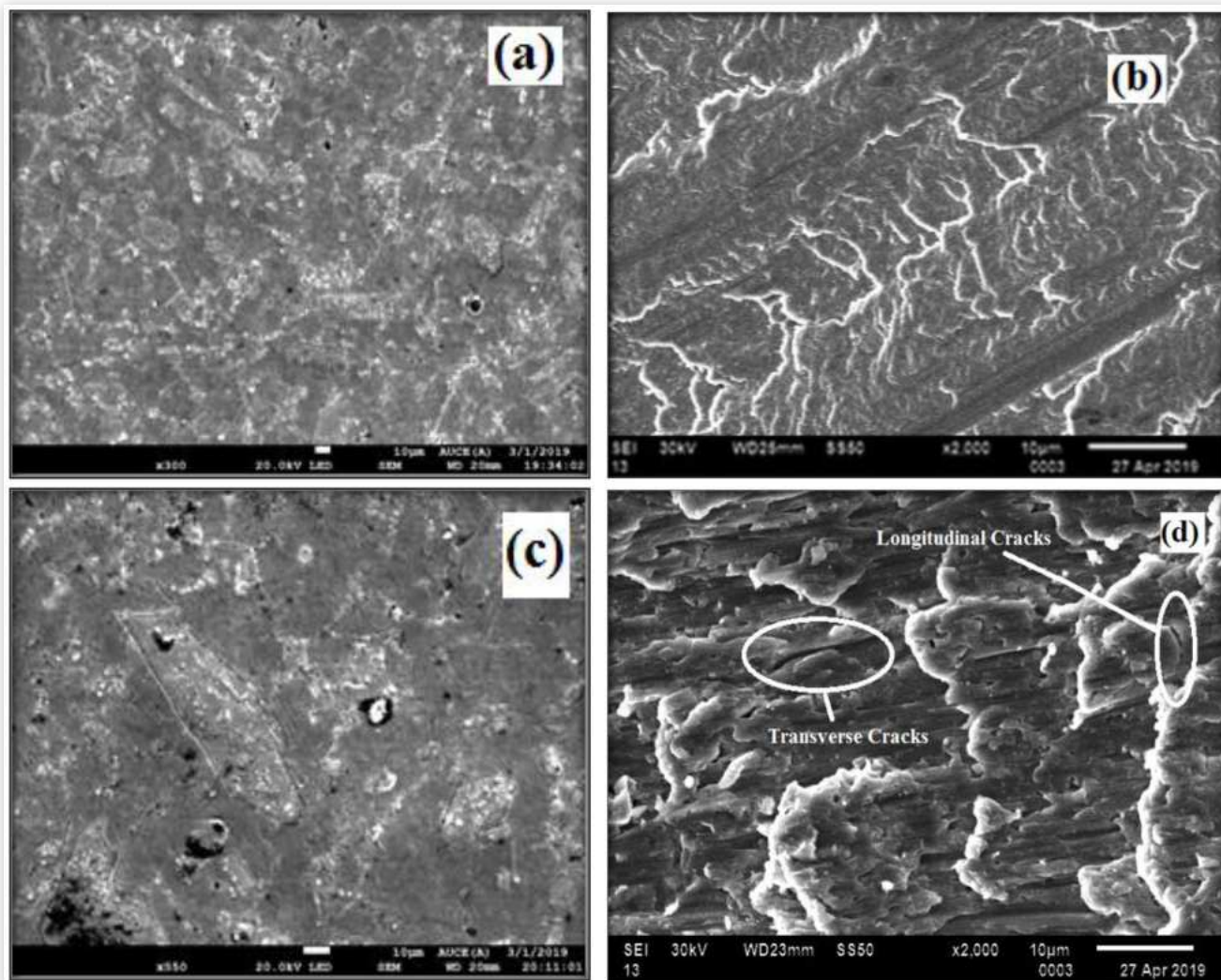
At long last, these cracks further propagate to produce finer debris. Figure 9 depicts a comparison in the size of in situ composite wear debris with different wt.% of TiB₂. The wear debris consists of mixed morphology of particles, with the dominant being the equiaxed type. This is mainly due to the interaction during the sliding wear between hard TiB₂ particles and coarse flaky debris. For the AA5754-2.5 wt.% TiB₂ composite, the size of the debris [Figure 9(a) and (b)] is marginally larger than that of the 5 wt.% and 7.5 wt.% TiB₂ composite [Figure 9(c), (d), (e), and (f)] on the same conditions.

Figure 8 depicts the rise in load also makes it possible to form finer debris. This is in contrast with many of the earlier

results where coarse debris is formed at higher loads [31]. A larger quantity of TiB₂ particles and higher loads are favored by the system, similar to a high energy ball milling, to generate finer debris. This is very much comparable to the previous outcomes. Thus, the transformation from mostly flaky in metal (Figure 9) to mostly equiaxed in composites in wear debris morphology (Figure 9) can significantly change the wear mechanism.

3.5. Pitting Corrosion

The pitting potential values of the master alloy and the in situ composites are given in Table 8. Figure 10 depicts the potentiodynamic polarization curves. TiB₂ formed due to the mixed salt route method greatly influences resistance to corrosion, when compared with the master composite, i.e., AA5754-0 wt.% TiB₂. The hard and tough particles are used as insulators and avoid the galvanic coupling between the matrix and the

FIGURE 8 (a) and (b) 10 N, (c) and (d) 40 N SEM micrographs of wear debris of AA5754 alloy at two different loads.

© SAE International

precipitates, thereby increasing resistance to pitting corrosion. There was a significant improvement of pitting corrosion resistance in 5 wt.% and 7.5 wt.% TiB_2 in situ composites. AA5754-5 wt.% TiB_2 has shown good corrosion resistance compared to other in situ composites. Figure 11 shows the optical micrographs of specimens after pitting corrosion testing. It is distinct that the formation of pits is very less in the in situ composites whose percentage of reinforcement is greater when compared to the master composite, i.e., AA5754-0 wt.% TiB_2 , which is a good sign of improved pitting corrosion resistance.

4. Conclusion

In the current study, AA5754- TiB_2 in situ composites were fabricated using the stir casting method. The mixed salt route

method was successfully adopted in the preparation of Al-Mg- $x\text{TiB}_2$ ($x = 2.5, 5, \text{ and } 7.5$ wt.%) composites. Based on the principles of Taguchi, the orthogonal array of L16 was considered to optimize the parameters such as Percentage of Reinforcement, Load, Sliding Speed, and Sliding Distance to minimize the WR of in situ composites and the master alloy. ANOVA was conducted to observe the significance of input parameters and their interactions. From the study, the following conclusions are drawn:

- TiB_2 was successfully synthesized in AA5754 through the mixed salt route method. Reinforcing TiB_2 in the matrix of AA5754 has a significant influence on the wear behavior of the material.
- Dry sliding tests at room temperature were conducted on in situ composites. There was a significant increase in the wear of these in situ composites. This is mainly due to

FIGURE 9 SEM photomicrographs of wear debris of Al5754-TiB₂ composites at three different loads of 10 N and 40 N for (a) and (b) 2.5 wt.%, (c) and (d) 5 wt.%, and (e) and (f) 7.5 wt.%.

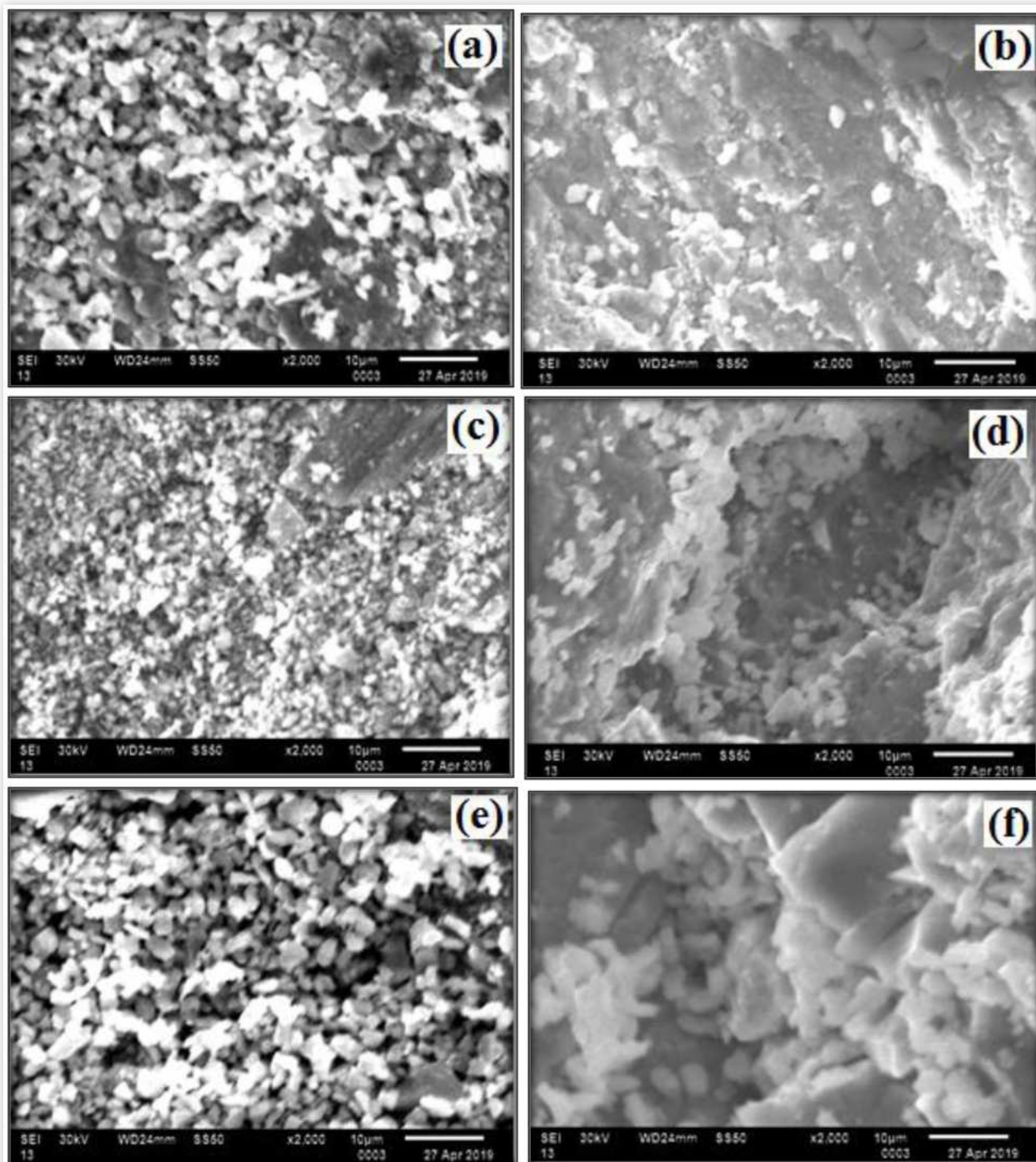


TABLE 8 Pitting potential values (mV) of base material and TiB₂-reinforced material.

% of reinforcement	E _{corr} (mV)	I _{corr} (mA/cm ²)	Corrosion rate (mm/year)
AA5754-0% TiB ₂	-1210	0.0142795	0.158787
AA5754-2.5% TiB ₂	-1395	0.0042139	0.046858
AA5754-5% TiB ₂	-1149.6	0.0004827	0.0053674
AA5754-7.5% TiB ₂	-1363.5	0.0126636	0.1408194

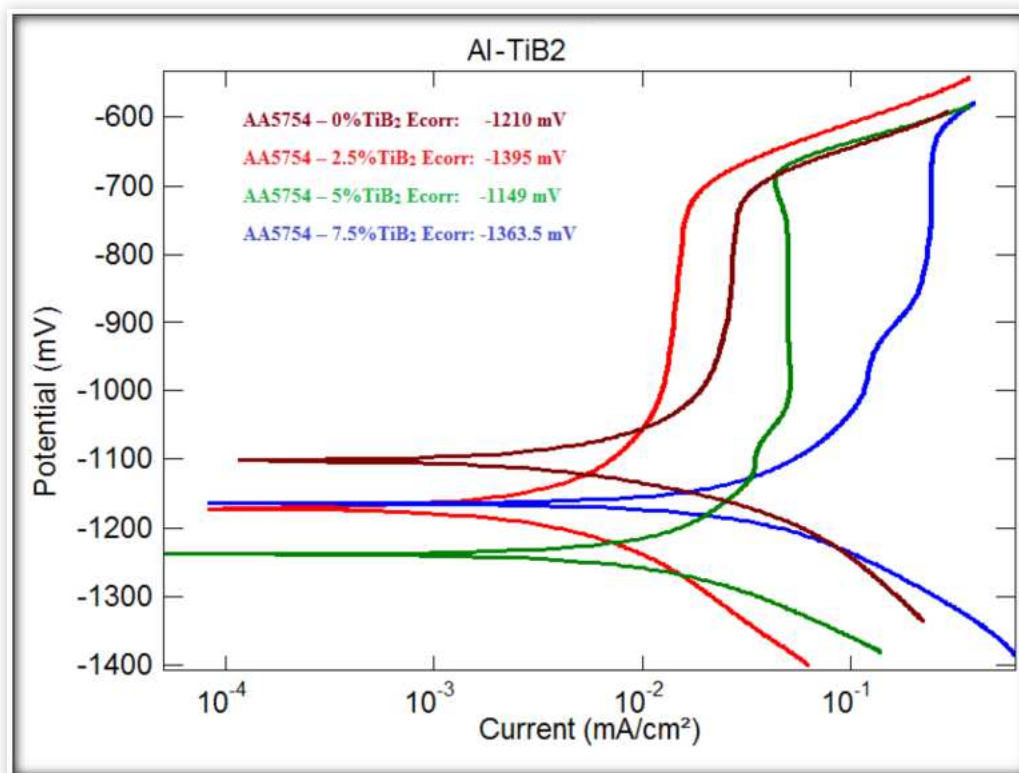
© SAE International

the synthesizing hard and tough particles of the TiB₂ in the AA5754 matrix and the formation of a protective layer between the pin and the counter face that enables wear resistance of the material.

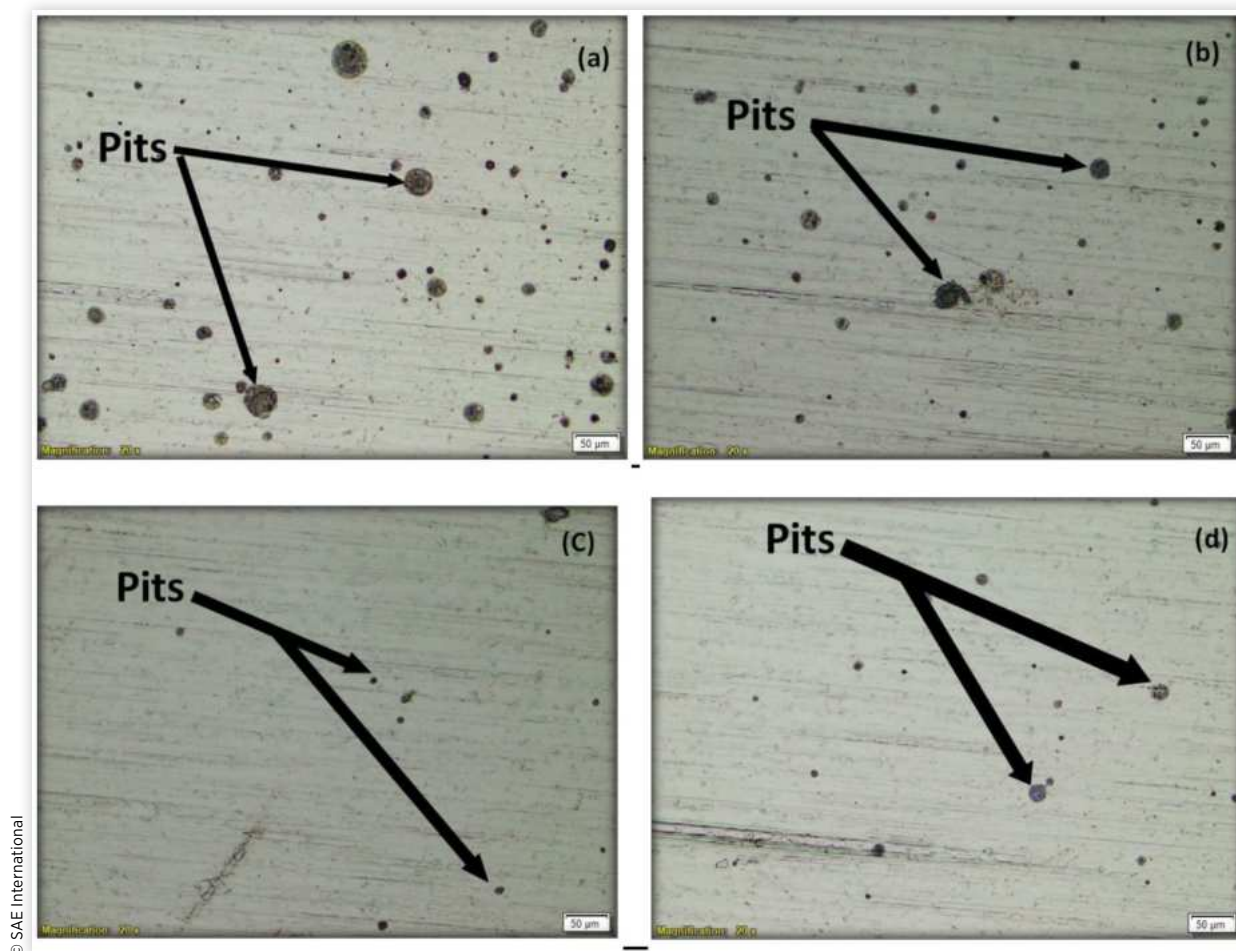
- Based on the literature, it is found that the wear rate is significantly increased when compared with the composites that are synthesized by using the ex situ method or any other conventional methods.
- The wear factor that has the greatest physical and statistical effect on the wear of the composites is the percentage of reinforcement. AA5754-xTiB₂ in situ composites present a contribution of the percentage of reinforcement (85.84%) and load (12.39%).
- The COF factor that has a great effect on the composites is the percentage of reinforcement. AA5754-xTiB₂ in situ

composites present a contribution of the percentage of reinforcement (86.03%) and load (12.42%).

- Interactions between sliding speed and sliding distance on the dry sliding are of a small percentage, yet they are considered statistically insignificant.
- The SEM micrographs clearly show the wear scars are being increased due to the increase in load and the formation of transverse and longitudinal cracks formed on the base material. But a remarkable difference has been observed on increasing the reinforcement of TiB₂ into the composites.
- The corrosion resistance of the material increases with increased TiB₂ content in the in situ composites. The potentiodynamic polarization curves and E_{corr} shows AA5754-5 wt.% TiB₂ has good corrosion resistance.

FIGURE 10 Potentiodynamic polarization curves.

© SAE International

FIGURE 11 Optical micrographs of base material and TiB₂-reinforced material after pitting corrosion test.

References

1. Kumar, S., Subramanya Sarma, V., and Murty, B.S., "A Statistical Analysis on Erosion Wear Behaviour of A356 Alloy Reinforced with In Situ Formed TiB₂ Particles," *Mater. Sci. Eng. A* 476:333-340, 2008.
2. Lakshmi, S., Lu, L., and Gupta, M., "In Situ Preparation of TiB₂ Reinforced Al Based Composites," *Journals of Materials Processing Technology* 73:160-166, 1998.
3. Venkata Subbaiah, K. and Bhanu Palampalle, K.B., "Microstructural Analysis and Mechanical Properties of Pure Al-GNPs Composites by Stir Casting method," *Inst. Eng. India Ser. C* 100(3):493-500, 2019.
4. Ramki, A., Brahma Raju, K., Venkatasubbaiah, K., Suresh, C., and Jagadish, K.E., "Microstructure and Hardness Characterization Behaviour of Al-Mg-TiB₂ In-Situ Composites," *IJITEE* 8(10):461-466, 2019.
5. Tisza, M. and Czinege, I., "Comparative Study of the Application of Steels and Aluminium in Lightweight Production of Automotive Parts," *International Journal of Lightweight Materials and Manufacture* 1:229-238, 2018.
6. Miller, W.S., Zhuang, L., Bottema, J., Wittebrood, A.J. et al., "Recent Development in Aluminium Alloys for the Automotive Industry," *Materials Science and Engineering A* 280:37-49, 2000.
7. Comez, N. and Durmus, H., "Mechanical Properties and Corrosion Behavior of AA5754-AA6061 Dissimilar Aluminum Alloys Welded by Cold Metal Transfer," *Journal of Materials Engineering and Performance* 29(6):3777-3784, 2019.
8. Jin, H., Saimoto, S., Ball, M., and Threadgill, P.L., "Characterisation of Microstructure and Texture in Friction Stir Welded Joints of 5754 and 5182 Aluminium Alloy Sheets," *Materials Science and Technology* 17:1605-1613, 2001.
9. Tjong, S.C. and Ma, Z.Y., "Microstructural and Mechanical Characteristics of In Situ Metal Matrix Composites," *Mater. Sci. Eng.* 49(113):R29, 2000.
10. Tjong, S.C. and Ma, Z.Y., "Microstructural and Mechanical Characteristics of In Situ Metal Matrix Composites," *Mater. Sci. Eng.* R29:49-113, 2000.

11. Aikin, R.M. Jr., "The Mechanical Properties of In-Situ Composites," *JOM* 49 8:35-39, 1997.
12. Kumar, S., Chakraborty, M., Subramanya Sarma, V., and Murty, B.S., "Tensile and Wear Behaviour of In Situ Al-7Si/TiB₂ Particulate Composites," *Wear* 265(1-2):134-142, 2008.
13. Tee, K.L., Lu, L., and Lai, M.O., "Wear Performance of In Situ Al-TiB₂ Composite," *Wear* 240:59-64, 2000.
14. Tyagi, R., "Synthesis and Tribological Characterization of In-Situ Cast Al-TiC Composites," *Wear* 259:569-576, 2005.
15. Wu, S.Q., Zhu, H.G., and Tjong, S.C., "Wear Behavior of In Situ Al-Based Composites Containing TiB₂, Al₂O₃ and Al₃Ti Particles," *Metall. Mater. Trans.* 30:243-247, 1999.
16. Wood, J.V., Davies, P., and Kellie, J.L.F., "Properties of Reactively Cast Aluminium-TiB₂ Alloys," *Mater. Sci. Technol.* 9:833-840, 1993.
17. Huang, M., Li, X., Yi, H., Ma, N., and Wang, H., "Effect of In Situ TiB₂ Particle Reinforcement on the Creep Resistance of Hypoeutectic Al-12Si Alloy," *Alloys Comp.* 389:275-280, 2005.
18. Schaffer, P.L., Arnberg, L., and Dahle, A.K., "Segregation of Particles and Its Influence on the Morphology of the Eutectic Silicon Phase in Al-7 wt.% Si Alloys," *Scripta Mater.* 54:677-682, 2006.
19. Yi, H., Ma, N., Zhang, Y., Li, X., and Wang, H., "Effective Elastic Moduli of Al-Si Composites Reinforced In Situ with TiB₂ Particles," *Scripta Mater.* 54:1093-1097, 2006.
20. Kumar, S., Subramanya Sarma, V., and Murty, B.S., "Influence of In-Situ Formed TiB₂ Particles on the Abrasive Wear Behaviour of Al-4Cu Alloy," *Mat. Sci. and Eng. A* 465(1-2):160-164, 2007.
21. Mandal, A., Chakraborty, M., and Murty, B.S., "Effect of TiB₂ Particles on Sliding Wear Behaviour of Al-4Cu Alloy," *Wear* 262(1-2):160-166, 2007.
22. Mandal, A., Maiti, R., Chakraborty, M., and Murty, B.S., "Effect of TiB₂ Particles on Aging Response of Al-4Cu Alloy," *Materials Science and Engineering: A* 386(1-2):296-300, 2004.
23. Selvam, J.D.R., Dinaharan, I., Vibin Philip, S., and Mashinini, P.M., "Microstructure and Mechanical Characterization of In Situ Synthesized AA6061/(TiB₂+Al₂O₃) Hybrid Aluminum Matrix Composites," *Journal of Alloys and Compounds* 740:529-535, 2018.
24. Afkham, Y., Khosroshahi, R.A., Rahimpour, S., Aavani, C. et al., "Enhanced Mechanical Properties of In Situ Aluminium Matrix Composites Reinforced by Alumina Nanoparticles," *Archives of Civil and Mechanical Engineering* 18:215-226, 2018.
25. Radhika, N., Subramanian, R., and Prasad, S.V., "Tribological Behaviour of Aluminium/Alumina/Graphite Hybrid Metal Matrix Composite Using Taguchi's Techniques," *Mineral & Mat. Characterization & Eng.* 10(5):427-443, 2011.
26. Sahin, Y., "Abrasive Wear Behaviour of SiC/2014 Aluminium Composite," *Tribol. Int.* 43:939-943, 2010.
27. Koksall, S., Ficici, F., Kayikci, R., and Savas, O., "Experimental Optimization of Dry Sliding Wear Behavior of In-Situ AlB₂/Al Composite Based on Taguchi's Method," *Mater Des* 42:124-130, 2012.
28. Kundu, S., Roy, B.K., and Mishra, A.K., "Study of Dry Sliding Behaviour of Aluminium/SiC/Al₂O₃/Graphite Hybrid Composite Using Taguchi Technique," *Int. Journal of Sci. and Res. Publication* 3:1-8, 2013.
29. Uvaraja, V.C. and Natarajan, N., "Optimization of Friction and Wear Behaviour in Hybrid Metal Matrix Composites Using Taguchi Technique," *Minerals and Mat. Characterization and Eng.* 11:757-768, 2012.
30. Lekatou, A., Karantzalis, A.E., Evangelou, A., Gousia, V. et al., "Aluminium Reinforced by WC and TiC Nanoparticles (Ex-Situ) and Aluminide Particles (In-Situ): Microstructure, Wear and Corrosion Behaviour," *Mat. and Des.*, 65:1121-1135, 2014.
31. Najafabadi, M.F., Golozar, M.A., Saidi, A., and Edris, H., "Wear Behaviour of Aluminium Matrix TiB₂ Composite Prepared by In Situ Processing," *Materials Science and Technology* 19(11):1531-1532, 2003.
32. Koksall, S., Ficici, F., Kayikci, R., and Savas, O., "Experimental Optimisation of Dry Sliding Wear Behaviour of In-Situ AlB₂/Al Composite Based on Taguchi's Method," *Mat. and Des.* 42:124-130, 2012.
33. Kumar, S., Sarma, V.S., and Murthy, B.S., "Influence of In-Situ Formed TiB₂ Particles on the Abrasive Wear Behaviour of Al-4Cu Alloy," *Mat. Sci. And Eng., A* 465:162-164, 2007.